Defined Sites of Interaction between Subunits E (Vma4p), C (Vma5p), and G (Vma10p) within the Stator Structure of the Vacuolar H^+-ATPase†

Richard P. O. Jones, Lyndsey J. Durose, John B. C. Findlay, and Michael A. Harrison*

School of Biochemistry and Microbiology, University of Leeds, Leeds LS2 9JT, United Kingdom

Received July 27, 2004; Revised Manuscript Received January 6, 2005

ABSTRACT: Vacuolar H^+-ATPases (V-ATPases) are multi-subunit membrane proteins that couple ATP hydrolysis to the extrusion of protons from the cytoplasm. Although they share a common macromolecular architecture and rotational mechanism with the F_1F_0-ATPases, the organization of many of the specialized V-ATPase subunits within this rotary molecular motor remains uncertain. In this study, we have identified sequence segments involved in linking putative stator subunits in the *Saccharomyces* V-ATPase. Precipitation assays revealed that subunits Vma5p (subunit C) and Vma10p (subunit G), expressed as glutathione-*S*-transferase fusion proteins in *E. coli*, are both able to interact strongly with Vma4p (subunit E) expressed in a cell-free system. GST-Vma10p also associated with Vma2p and Vma1p, the core subunits of the ATP-hydrolyzing domain, and was able to self-associate to form a dimer. Mutations within the first 19-residue region of Vma4p, which disrupted interaction with Vma5p in vitro, also prevented the Vma4p polypeptide from restoring V-ATPase function in a complementation assay in vivo. These mutations did not prevent assembly of Vma5p (subunit C) and Vma2p (subunit B) into an inactive complex at the vacuolar membrane, indicating that Vma5p must make multiple interactions involving other V-ATPase subunits. A second, highly conserved region of Vma4p between residues 19 and 38 is involved in binding Vma10p. This region is highly enriched in charged residues, suggesting a role for electrostatic effects in Vma4p−Vma10p interaction. These protein interaction studies show that the N-terminal region of Vma4p is a key factor not only in the stator structure of the V-ATPase rotary molecular motor, but also in mediating interactions with putative regulatory subunits.

The vacuolar H^+-ATPases (V-ATPases)[1] are a family of multi-subunit membrane protein complexes that directly couple the free energy of ATP hydrolysis to the transmembrane movement of protons. Found in virtually every type of eukaryotic cell, they function to maintain the acidic internal environment of intracellular compartments or contribute to pH homeostasis by extruding protons across the plasma membrane (*1*, *2*). It is now well established that the V-ATPase shares not only a similar macromolecular structure with the ATP-synthesizing F_1F_0-ATPase (*1*) but also a common rotational mechanism (*3*−*5*). Both species of ATPase comprise a soluble domain (V_1 or F_1), which houses the nucleotide binding sites, coupled both physically and mechanistically to an integral membrane domain (V_0 or F_0), which is the proton transporter. The V-ATPase-soluble domain contains subunits designated A−H in the probable stoichiometry $A_3B_3CDEFG_2H$, while the smaller membrane domain contains integral membrane subunits a, c, c′, and c″ and the membrane-associated subunit d with a likely $ac_4c'c''d$ stoichiometry (*6*, *7*). Underlining the evolutionary relationship between F- and V-ATPases, a number of core subunits of the two complexes share significant sequence similarity: the V_1 domain subunits A and B, which contribute to both catalytic and noncatalytic ATP binding sites, are closely related to the β- and α-subunits of the F-ATPase, respectively (*8*, *9*). Within the V_0 membrane domain, the 16-kDa proton-translocating subunit c (and the related subunits c′ and c″) appears to have evolved as a tandem repeat of the same ancestral polypeptide that gave rise to the 8-kDa subunit c of the F-ATPase (*10*). Even the apparently quite different a-subunits of the two ATPase show highly localized sequence similarity within the transmembrane regions that contribute to the proton translocation function. Of the remaining V-ATPase subunits, only subunit G bears any resemblance at the primary structure level to an F-ATPase equivalent. It corresponds to the extra-membranous region of the b-subunit of the F_0 domain (*11*, *12*). Lack of sequence similarity between the remaining V-ATPase subunits and any F-ATPase components renders it impossible to make further inferences about functions of individual V-ATPase subunits. However, core V_1 and F_1 complexes containing subunits A_3B_3DF and $\alpha_3\beta_3\gamma\epsilon$, respectively, are both competent for catalysis, measured as ATP-dependent rotation (*4*, *13*). The clear implication is that the V-ATPase D and F subunits are functional homologues of the F-ATPase γ- and ϵ-subunits. This functional equivalence infers that these V-type subunits might adopt folds similar to those of their F-ATPase equivalents, even though they bear no comparison at the level of primary structure. Such inferences are supported by

† This work was supported by grants from the UK BBSRC (24/b14097) and European Union Framework V (QLRT-1999-31801).

* To whom correspondence should be addressed. Telephone: (+44) 113 3437766. Fax: (+44) 113 3433167. E-mail: m.a.harrison@leeds.ac.uk.

[1] Abbreviations: V-ATPase, vacuolar H^+-translocating ATPase; F-ATPase, F_1F_0-ATP synthase; GST, glutathione-*S*-transferase; ORF, open reading frame; *VMA*, vacuolar membrane ATPase subunit.

10.1021/bi048402x CCC: $30.25
Published on Web 02/10/2005

secondary structure analyses of recombinant V-ATPase subunits (*14*, *15*).

In the case of the F-ATPase rotary motor, sequential force generating steps requiring the hydrolysis of ATP are translated into rotation of a central spindle structure consisting of the γ and ϵ subunits (*13*). Because this structure is fixed to subunit c, torque acting on the $\gamma-\epsilon$ spindle drives rotation of the oligomeric subunit-c complex within the membrane (*16*). The corresponding spindle structure within the V-ATPase is the subunit D- subunit F complex (*4*), similarly coupled to the subunit-c oligomer within the bilayer (*3*, *17*). In both ATPase species, proton translocation is postulated to occur at the dynamic interface between the subunit-c oligomer and the single copy subunit a. To achieve the relative movement of the a and c subunits, the rotary motor model requires a stator structure to fix subunit a relative to the ATP-hydrolyzing domain. This structure is clearly visible as a second, peripheral stalk in electron microscopy images of both the V- and the F-ATPases (*18*). In the bacterial F-ATPase, this structure consists of two copies of subunit b and the δ-subunit (*19*), whereas in the V-ATPase contributions from subunits G, E, C, and H, d and a are all possible. However, the relationship between subunit G and subunit b of the F-ATPase points to this V-ATPase subunit being a core component of the stator (*3*, *11*).

Information about subunit interactions within the stator substructure of the V-ATPase has come from a variety of biochemical and proteomic approaches (*20*−*24*). Early studies using chemical cross-linkers showed that subunit E is close to subunits C, G, H, and the soluble domain of subunit a (*20*). Subunit E also forms a complex with subunit G in vivo (*21*), associates with subunit C in immunoprecipitation experiments (*22*) and interacts with heterologously expressed subunit H via its N-terminal region (*23*). Targeted cross-linking studies indicate that sites dispersed across the external surface of subunit B also contact subunit E (*24*).

The aim of this study is to increase the level of resolution regarding interactions between candidate stator subunits in the *Saccharomyces* V-ATPase. With this in mind, we have analyzed associations between heterologously expressed, highly purified Vma5p and Vma10p (the *Saccharomyces* forms of subunits C and G, respectively) and the other yeast V-ATPase-soluble domain subunits expressed in vitro. By looking at the influence of deletions and site-specific mutations on the observed protein−protein associations, we have been able to identify specific sites that are involved in establishing some key subunit interactions. The importance of these sites in the overall organization of the active V-ATPase was confirmed by testing the effects of mutations on assembly and function of the holoenzyme in yeast. The influence of these sites on subunit interactions in vivo suggests that they may be crucial to the physical link between V-ATPase domains and, therefore, important in controlling the functional coupling between ATP hydrolysis and proton translocation.

EXPERIMENTAL PROCEDURES

Molecular Biology and Mutagenesis. CDNAs or each *VMA* gene were obtained by PCR from yeast genomic DNA with primers identified using the primer design facility at the *Saccharomyces* Genome Database (http://seq.yeastgenome.org/cgi-bin/web-primer), detailed in the Supporting Information. PCR products were subcloned using topoisomerase-activated pCR-II-Blunt (Invitrogen). Authenticity of the cDNAs was confirmed by DNA sequencing (Lark Industries Inc., Saffron Walden, UK). For expression of GST fusion proteins, the *VMA5* and *VMA10* cDNAs were modified by PCR so that they incorporated 5′ *Bam*HI and 3′ *Not*I restriction sites. These sites allowed in-frame subcloning of *VMA cDNAs* at the 3′ end of the GST coding sequence in the vector pGEX-6P3 (Amersham Biosciences). Correct in-frame transition from GST to each *VMA* coding sequence was confirmed by DNA sequencing. Complete primer sequences used to prepare the GST fusion constructs are listed in the accompanying Supporting Information.

The T7 RNA polymerase recognition sequence of pCR-II-Blunt is some 70 base pairs from the site of insertion of cDNAs and drives only very small amounts of expression in vitro. To optimize expression of V-ATPase subunits, cDNAs for each subunit and for truncated and mutated forms of Vma4p were modified by PCR such that they incorporated a 20 base pair T7 site immediately 5′ to the *VMA* coding sequence, separated from the initiating ATG by a six base pair spacer (CCCACC) only. This spacer sequence and initiating codon constitute a consensus Kozak sequence (ACCAUGG), maximizing expression. Site-directed mutants of Vma4p were generated via the QuikChange method (Stratagene) using as template the wild-type *VMA4* construct with incorporated T7-Kozak sequence as outlined above. Primers used in the mutagenesis experiments are detailed in the Supporting Information. Mutations were confirmed by DNA sequencing.

Expression and Purification of GST Fusion Proteins. For expression and purification of GST fusion proteins, each pGEX construct was used to transform *E. coli* strain BL21, and resulting transformants were grown overnight in Luria-Bertani medium supplemented with 50 μg/mL ampicillin at 37 °C. When the culture reached an optical density of 0.5 at 630 nm, expression was induced by the addition of IPTG (200 μM), with incubation for a further 4 h. Cells were harvested by centrifugation (5000*g* for 10 min) and concentrated 100-fold with respect to the culture volume in Buffer A (20 mM phosphate buffer, 150 mM NaCl, pH 7.2, supplemented with 50 μg/mL RNase A (Sigma) and complete EDTA-free protease inhibitor cocktail (Roche Diagnostics, Mannheim, Germany)). Cells were lysed by extrusion through a French pressure cell (20 000 psi), and the cell lysate was clarified by centrifugation at 60 000*g* for 1 h at 4 °C before being applied to glutathione Sepharose 4FF (Amersham Biosciences, Uppsala, Sweden). After washing with Buffer A, fusion protein was eluted from the sepharose support by washing with a solution of reduced glutathione (10 mM) in 50 mM Tris HCl pH 8.0. Fractions containing the fusion protein were pooled and concentrated in centrifugal concentrators (VivaSpin, Viva Sciences) equipped with 5-kDa molecular mass cutoff filters. A process of 20-fold concentration followed by 20-fold re-dilution in Buffer A, repeated four times, was used to remove glutathione from the solution of fusion protein. Finally, the fusion proteins were concentrated 20-fold and stored at −20 °C.

Expression of V-ATPase Subunits in Vitro. Individual V-ATPase subunits were expressed in vitro using the TNT coupled rabbit reticulocyte lysate system (Promega, Madison,

WI) and labeled with ^{35}S-methionine (20 μCi per reaction: specific activity 1000 Ci/mmol; PerkinElmer Life Sciences Inc., Boston, MA). To probe for interactions between radiolabeled V-ATPase subunits expressed in vitro and the GST-Vma5p/Vma10p fusion proteins, translation mixtures (50 μL) were incubated overnight on a blood roller at 4 °C with GST-*VMA* fusion protein (0.2 nmol) or GST (0.4 nmol) and glutathione Sepharose beads (60 μL of 50% slurry in Buffer B: 20 mM phosphate buffer, 150 mM NaCl pH 7.2 with 1% w/v Triton X-100). The beads were recovered by centrifugation (500*g*, 5 min), washed five times with 10 volumes of Buffer B, and then boiled for 10 min in 20 μL of SDS-PAGE sample preparation buffer (5% SDS, 50 mM Tris HCl pH 6.8, 20% glycerol, 5% v/v 2-mercaptoethanol). After centrifugation, 12 μL of the supernatant was analyzed by SDS-PAGE on 12.5% acrylamide gels. For direct analysis of in vitro translation, translation mixtures (5 μL) were mixed with 6-fold concentrated SDS-PAGE sample buffer (1 μL), and all 6 μL was loaded onto gels. The gels were stained and fixed in 30% methanol/10% acetic acid with 0.5% w/v Coomassie Brilliant Blue, destained, and analyzed by autoradiography after drying under vacuum.

Expression and Functional Screening in Saccharomyces cerevisiae. For expression in yeast, *VMA4* cDNAs were subcloned into the galactose-inducible shuttle vector pYES2 (Invitrogen). A haploid yeast strain (BY7349, genotype *Mat*α, *leu2*Δ0, *lys2*Δ0, *ura3*Δ0, obtained from Open Biosystems, Huntsville, AL) in which the *VMA4* gene is disrupted by insertion of a kanamycin resistance cassette was transformed with the pYES2 constructs using the lithium acetate method (*25*). Transformants were selected on the basis of complementation of the *ura3* deletion by the *URA3* marker in pYES2, in the presence of the antibiotic G418 (100 μg/mL). Disruption of *VMA* genes in yeast is characterized by a conditional lethal pH-sensitive phenotype (*26*, *27*), and complementation of the *vma4* mutation is manifested as restored ability to grow at pH 7.5. Cells transformed with individual *VMA4* constructs were therefore tested for complementation of the *vma4* mutation by plating onto yeast extract-peptone media buffered to pH 5.5 or pH 7.5 with 50 mM MOPS/50 mM MES, and supplemented with 1% glucose or 1% galactose/1% raffinose. Growth at pH 7.5 was scored relative to that of a yeast strain transformed with plasmid harboring the wild-type *VMA4* cDNA.

Assay of V-ATPase Assembly in Vivo. Assembly of the V-ATPase was analyzed by immunoblotting for the presence of soluble domain subunits Vma2p (subunit B) and Vma5p (subunit C) associated with the vacuolar membrane. Cells were grown in synthetic minimal medium (0.67% yeast nitrogen base, 50 mM MOPS/50 mM MES pH 5.5, 40 μg/mL lysine, 40 μg/mL leucine, 100 μg/mL G418, 1% galactose, 1% raffinose) to late log phase and were harvested by centrifugation. EDTA-washed vacuolar membrane vesicles were isolated by the method of (*28*). Proteins were separated by SDS-PAGE, electrophoretically blotted onto PVDF membrane, and probed with anti-Vma2p mouse monoclonal antibody (Molecular Probes, Eugene, OR) or anti-Vma5p rabbit polyclonal antisera (generously donated by Prof. Tom Stevens, University of Oregon). Blots were developed using the appropriate HRP-conjugated secondary antibody and chemiluminescent substrate (Boehringer, Mannheim, Germany). Protein assay was performed using the BCA method with BSA as standard.

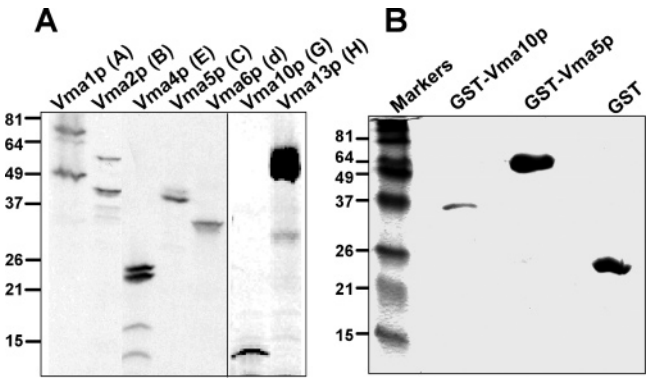

FIGURE 1: Expression of *Saccharomyces* V-ATPase subunits. (A) Individual subunits were expressed in vitro using a coupled transcription/translation system in the presence of ^{35}S-methionine, separated by SDS-PAGE and detected by autoradiography (48 h exposure). Gene product designations from *Saccharomyces* are shown, with the generic subunit letter designations in parentheses. Polypeptide species shorter than full-length correspond to translation products initiated at internal AUG codons. Because of the scarcity of methionine residues in Vma10p, the region of the gel containing this subunit was exposed to autoradiographic film for 10 days. (B) GST-Vma10p, GST-Vma5p, and GST proteins were expressed in *E. coli*, affinity purified on glutathione sepharose and analyzed by SDS-PAGE. Positions and masses of markers (in kDa) are shown.

RESULTS

1. Expression of V-ATPase Subunits in E. coli and in Cell-Free Systems. CDNAs equivalent to the ORF of each *Saccharomyces VMA* gene were cloned by PCR from genomic DNA and tested for their capacity to support coupled transcription/translation in vitro. Polypeptides radiolabeled with ^{35}S-methionine were manufactured using a T7 RNA polymerase-based transcription system coupled to translation in a rabbit reticulocyte lysate. For each individual *VMA* cDNA, the largest translation product had a molecular mass corresponding to that deduced from the corresponding nucleotide sequence (Figure 1A). For a number of subunits, shorter translation products were also seen (for example, Vma2p and Vma4p in Figure 1A). The masses of these corresponded exactly to the values predicted for polypeptides produced by initiation of translation at internal AUG codons. Analysis of the *VMA* gene sequences confirms that polypeptides of these masses could not be produced as artifacts by reading frame shift, and that they are therefore authentic, but N-terminally truncated, versions of *VMA* subunits. Adjustment of parameters such as the amount of plasmid in the translation mixture and length of time of translation had no effect on the relative levels of these products (data not shown). Note also that the 120-kDa translation product of the *VMA1* cDNA undergoes posttranslational splicing and re-ligation in vitro to produce the 70-kDa subunit A and 50-kDa intein polypeptides (*29*).

Expression of Vma5p and Vma10p as N-terminal fusions with GST in *E. coli* resulted in the production of soluble 70-kDa and 40-kDa polypeptides, respectively (Figure 1B). Verification of the purified polypeptides as full-length was confirmed by mass spectrometry after proteolytic cleavage and removal of the GST component (data not shown). The purified polypeptides were soluble and monodisperse, as judged by size exclusion chromatography, and folded with secondary structure as determined by CD spectroscopy (*30*).

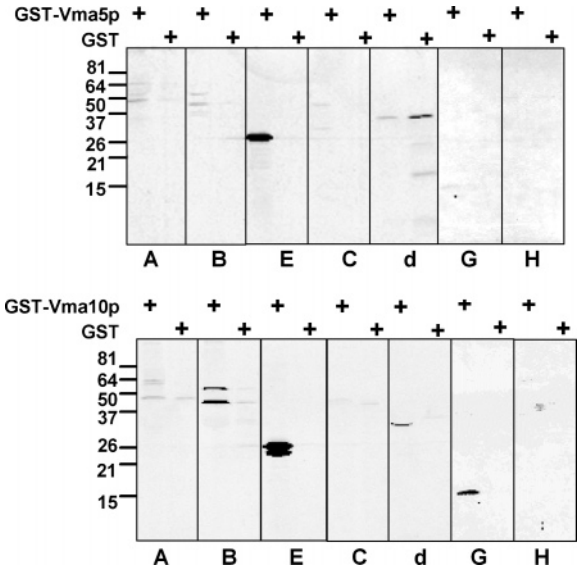

FIGURE 2: Recombinant Vma5p and Vma10p fusion proteins make specific interactions with V-ATPase subunits expressed in vitro. Individual ^{35}S-labeled polypeptides, expressed as in Figure 1A, were incubated with GST-Vma5p (upper panel) or GST-Vma10p (lower panel) fusion proteins. The resulting complexes were extracted by binding to glutathione sepharose and analyzed by SDS-PAGE and autoradiography (48 h exposure). Association with GST alone provided a test of nonspecific binding. Positions and masses of markers (in kDa) are shown. Single letter designations of individual expressed V-ATPase subunits are given at the bottom of each lane.

2. Analysis of V-ATPase Subunit Interactions in Vitro. Precipitation experiments exploiting the affinity of the GST component of the Vma5p and Vma10p fusion proteins for glutathione sepharose were used to assess interactions between these subunits and the other soluble yeast V-ATPase subunits expressed in vitro (Figure 2). Formation of heteromeric complexes incorporating ^{35}S-labeled polypeptides was detected by SDS-PAGE and autoradiography, with specificity of interactions being verified by testing for interactions between the radiolabeled subunits and recombinant GST alone. Crucially, a strong and highly specific interaction between GST-Vma5p and Vma4p (subunit E) was consistently detected using this assay (Figure 2, upper panel). Only the full-length Vma4p polypeptide formed a complex with GST-Vma5p, despite the presence of truncated forms of Vma4p in the translation product mixture. Interaction between GST-Vma5p and Vma6p (subunit d) was also detected (Figure 2), but discounted, because it appeared to be a nonspecific interaction mediated via the GST component.

GST-Vma10p also interacted weakly with Vma1p (subunit A), but made relatively strong and specific interactions with both full-length Vma2p (subunit B) and an apparent truncation of Vma2p (Figure 2, lower panel). This truncated Vma2p is presumed to be missing the N-terminal 107 residues preceding the second methionine in the amino acid sequence. GST-Vma10p also made weak but specific interactions with Vma6p (subunit d) and with itself, confirming previous observations that this subunit can assemble as a dimer (*31*). As with GST-Vma5p, the recombinant Vma10p fusion protein interacted most strongly with Vma4p (subunit E, Figure 2, lower panel). Unlike Vma5p, it appeared to interact equally strongly with a truncated version of Vma4p, which is approximately 2-kDa smaller than the full-length translation product. This product is presumed to have arisen as a consequence of translation initiating erroneously at a Met^{20} of Vma4p (see Figure 8). The Vma8p (subunit D) and Vma7p (subunit F) polypeptides, already defined as components of the ATPase "rotor" structure (*4*), behaved quite differently in the GST pull-down assay. Vma7p did not interact with GST-Vma10p, GST-Vma5p, or GST, whereas Vma8p made nonspecific interactions equally with all three proteins, presumably via the GST component (data not shown).

Figure 2 clearly shows that both Vma5p and Vma10p make strong interactions with Vma4p and that they discriminate between different truncated versions of the polypeptide. To examine these associations in more detail, we constructed five truncated versions of Vma4p (Figure 3) and tested them for interaction with GST-Vma5p and GST-Vma10p. The truncations included removal of all residues N-terminal to the second (Δ1−19) or third (Δ1−69) methionine in the Vma4p sequence, and removal of the first 38 residues of the subunit (Δ1−38). Secondary structure prediction algorithms (*32*) predict with high probability that Vma4p comprises two domains: an N-terminal half containing perhaps as few as one or two extended α-helices, with a C-terminal half comprising a mixture of short α-helical and *β*-turn structures (Figure 3). In line with these predictions, we have generated constructs corresponding to the first 111 (Δ112−223) or the last 123 (Δ1−110) residues of Vma4p, allowing independent expression of each putative domain.

FIGURE 3: Strategy for Vma4p truncation. Secondary structure of the 233-residue *Saccharomyces* Vma4p is predicted to comprise an extended α-helical domain within the N-terminal 111 residues and a mixed domain of short regions of α-helix (open rectangles) and *β*-structure (shaded rectangles) within the C-terminal 122 residues. Truncated forms of Vma4p were constructed such that each putative domain could be expressed separately. Truncations were also constructed such that the first (Met^{20}) or second (Met^{70}) internal methionines of Vma4p became the N-terminal residues. In addition, a form of Vma4p was constructed in which the N-terminal 38 residues were deleted. This region between Met^{20} and Lys^{38} contains a sequence that is highly conserved between eukaryotic species (see Figure 8).

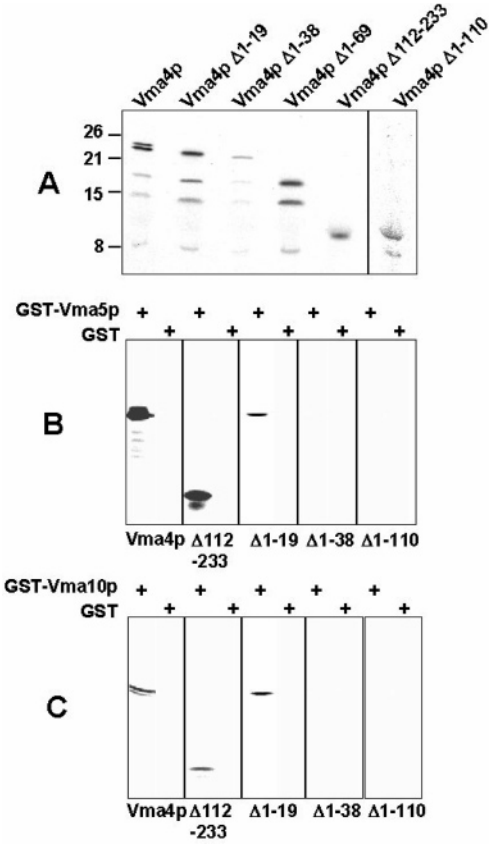

FIGURE 4: Truncated forms of Vma4p show differential interaction with Vma10p and Vma5p. (A) Truncated Vma4p polypeptides, expressed in vitro and labeled with ^{35}S-methionine, were analyzed by SDS-PAGE and autoradiography. Truncated versions of Vma4p, starting at Met^{20} or Met^{70} of the wild-type sequence, have masses corresponding to those of polypeptides produced by translational mis-start, which are present in the full-length Vma4p translation mixture. Positions and masses (in kDa) of markers are indicated. Translation mixtures in (A) were incubated with (B) GST-Vma5p or (C) GST-Vma10p, and resulting complexes were pulled down via interaction with glutathione sepharose. In each case, precipitation in the presence of GST was used to test for nonspecific binding. Following separation on SDS-PAGE, autoradiograms shown in A, B, and C were generated after 48 h exposure. Areas of gels containing the C-terminal region of Vma4p (Vma4pΔ1−110) were exposed for 10 days.

All of the truncated Vma4p polypeptides could be expressed in vitro (Figure 4A). Expression of the Δ1−19 and Δ1−69 truncations gave polypeptides that had masses identical to those of the translation products presumed to be made as a result of translational mis-starts from the full-length Vma4p mRNA (Figure 4A). Each truncated form of Vma4p was tested for interaction with GST-Vma5p and GST-Vma10p in precipitation assays (Figure 4B,C). Association of Vma5p with Vma4p was significantly reduced by removal of the N-terminal 19 residues of Vma4p, and interaction between these two subunits was abolished completely by the loss of the first 38 residues of Vma4p (Figure 4B). The importance of the N-terminal region of Vma4p for its interaction with Vma5p is underlined by the observation that the Vma4pΔ112−233 polypeptide retains the ability to bind strongly to Vma5p, whereas the C-terminal region of the subunit (Figure 4B: Vma4pΔ1−110) does not bind Vma5p. In contrast, interaction between Vma4p and GST-Vma10p was unaffected by deletion of the N-terminal 19 residues of Vma4p (Figure 4C). Interaction between the polypeptides was, however, completely abolished by removal of residues 1−38 of Vma4p. As seen with the Vma5p/Vma4p interaction, the N-terminal region of Vma4p ((Vma4pΔ112−223) retains the capacity to bind strongly to Vma10p, whereas the C-terminal region (Vma4pΔ1−110) does not (Figure 4C). These data clearly show that adjacent, but distinct, regions at the N-terminus of Vma4p show discriminatory binding of Vma5p and Vma10p.

3. Influence of Site-Specific Mutations on Vma4p/Vma5p Interactions in Vitro. To increase resolution of the Vma4p binding site for Vma5p, we assessed the effects of modifying amino acids in the region of Vma4p between residues 1−20 on the interaction between mutant polypeptides expressed in vitro and GST-Vma5p (Figure 5). Mutations within this region did not influence overall levels of expression in vitro (data not shown), but some amino acid changes did affect association between Vma4p and Vma5p. These apparent differences were not due to degradation of the in vitro translated protein, because the integrity of the radio-labeled polypeptides was not affected after incubation with the GST fusion protein (data not shown). With the exception of the mutation Thr^{9}→Ala (Figure 5: T9A), shifting amino acid side-chain characteristics from polar to hydrophobic (for example, Asn^{11}→Ala, Gln^{12}→Ala, Asp^{15}→Ala) had no significant effect on Vma4p/Vma5p interaction (Figure 5: N11A, Q12A, D15A). Similarly, alteration of the charge properties of residues such as Glu^{16}→Lys and Lys^{19}→Glu substitutions (Figure 5: E16K, K19E) had no effect on the interaction between the subunits. Replacement of Pro^{10} by alanine (Figure 5: P10A) did partially inhibit association, presumably mediated through localized changes in secondary structure within Vma4p. The most profound effects on Vma4p/Vma5p association were observed when hydrophobic residues were replaced by amino acids with charged side chains, such as in the case of Leu^{8}→Asp (Figure 5: L8D), Val^{13}→Glu (V13E), Leu^{17}→Asp (L17D), and by the substitution Met^{20}→Ala (M20A). These observations point to a role for hydrophobic interaction in driving and maintaining association between Vma4p and Vma5p. Consistent with secondary structure predictions for Vma4p (see Figure 3), these residues show broadly α-helical periodicity within the Vma4p amino acid sequence.

4. Effects of Vma4p Mutations on V-ATPase Function in Vivo. Mutant forms of *VMA4* were tested for their ability to abolish the pH-sensitive conditional lethal phenotype of a yeast strain carrying a disrupted *VMA4* gene. The basis for this complementation assay is shown in Figure 6. For growth at pH 5.5, V-ATPase function is not essential and cells will grow even in the absence of a functional *VMA4* gene (*26*). For growth at pH 7.5, assembly of an active V-ATPase is required, which in turn depends on expression of a functional Vma4p (*27*, *33*). In this study, Vma4p polypeptides are encoded episomally on the plasmid pYES2, from which expression is driven by the galactose-inducible *GAL1* promoter. Thus, recovery of growth at pH 7.5 should also be galactose-dependent if it is based on Vma4p expression from pYES2. To ensure that growth is dependent solely on plasmid-based expression, cells are tested for growth at pH 7.5 on media containing glucose. Under these conditions, the *GAL1* promoter of pYES2 is inactive and Vma4p is therefore not expressed. Consequently, there should be no complementation of the conditional lethal phenotype and no

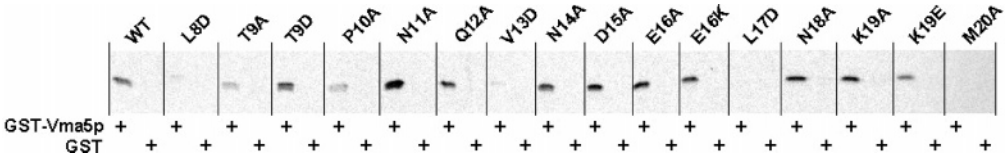

FIGURE 5: Mutation of specific residues within the N-terminal region of Vma4p influences interaction with Vma5p. Mutant Vma4p polypeptides, containing specific amino acid changes within the N-terminal 20 residue region, were expressed in vitro in the presence of ^{35}S-methionine. The capacity of each mutant Vma4p polypeptide to form a complex with Vma5p was assessed by GST pull-down assay, with stable Vma4p/GST-Vma5p complexes isolated by interaction with glutathione sepharose. Binding of mutant Vma4p polypeptides to GST was used to control nonspecific interactions. Note that Vma5p binds predominantly the full-length Vma4p translation product. Autoradiograms of SDS-PAGE gels were developed after 72 h exposure.

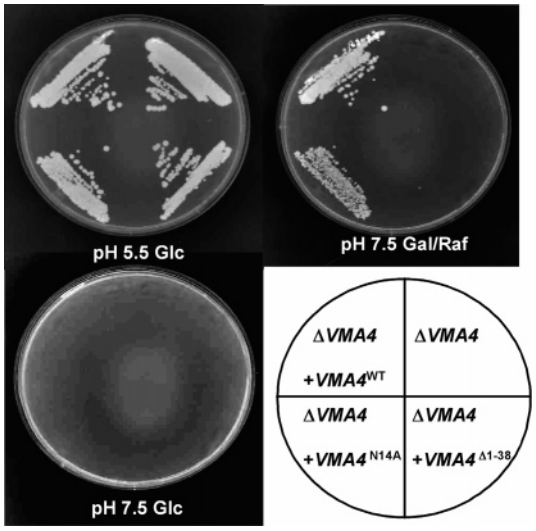

FIGURE 6: Assay of functionality of *VMA4* mutants in vivo. *VMA4*-deleted *Saccharomyces* cells (Δ*VMA4*) were transformed with pYES2 plasmids carrying mutant forms of *VMA4*, each capable of galactose-induced expression of the corresponding mutant Vma4p polypeptide. In this assay, recovery of V-ATPase function is indicated by restored growth at pH 7.5 in the presence of the inducer galactose, reflecting a loss of the pH-sensitive conditional lethal *vma* phenotype. Δ*VMA4* + *VMA4*^{WT}, Δ*VMA4* + *VMA4*^{N14A}, and Δ*VMA4* + *VMA4*$^{Δ1-38}$ indicate Δ*VMA4* cells transformed with plasmids carrying cDNAs for wild-type *VMA4*, Asn^{14}→Ala mutant *VMA4*, or *VMA4* deleted for the N-terminal residues 1−38, respectively. A complete set of data derived using this assay is given in Table 1.

growth at pH 7.5. In this complementation assay, none of the truncated forms of Vma4p were able to restore growth at pH 7.5 (Table 1), suggesting that these polypeptides are unable to support assembly of a functional V-ATPase. Similar analysis of the site-specific mutant forms of Vma4p showed that mutations Val^{13}→Asp, Leu^{17}→Asp, and Met^{20}→Ala also blocked the recovery of V-ATPase function seen in cells transformed with plasmid carrying the wild-type *VMA4* (Table 1). Expression of Vma4p carrying the mutation Leu^{8}→Asp was able to support only very weak growth at pH 7.5 (colonies <1 mm diameter after 12 days) (Table 1). As with the N-terminally truncated forms of Vma4p, failure to recover function implies compromised V-ATPase assembly, consistent with the observed effects of these mutations on Vma4p−Vma5p interactions in vitro (Figures 4 and 5). The charge shift mutation Lys^{19}→Glu also prevented recovery of V-ATPase function in vivo, although this mutation did not appear to completely inhibit the Vma5p−Vma4p interaction in vitro (Figure 5).

5. Effects of Vma4p Mutations on V-ATPase Assembly at the Vacuolar Membrane. Although failure of the mutant Vma4p polypeptides to support growth at pH 7.5 indicates

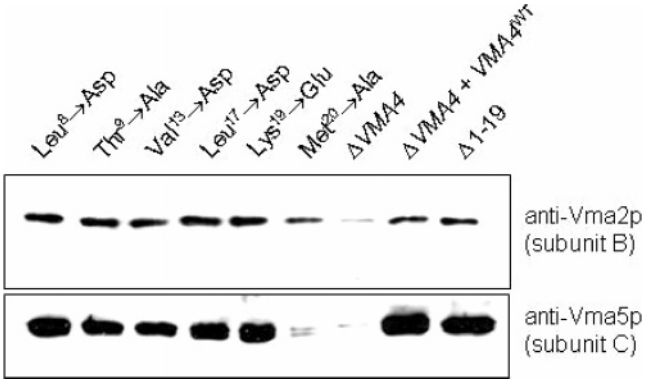

FIGURE 7: Effects of Vma4p mutations on assembly of the V-ATPase. Vacuolar membranes were isolated from cells expressing forms of Vma4p carrying site-specific mutations within the N-terminal 20 residue region, or deleted for the first 19 residues (Δ1−19) and compared to membranes isolated from the *VMA4*-deleted strain before (Δ*VMA4*) and after transformation with a plasmid carrying the wild-type *VMA4* (Δ*VMA4* + *VMA4*^{WT}). Vacuolar membrane proteins (10 μg total in each lane) were separated by SDS-PAGE and immunoblotted. Blots were developed with antibodies against the soluble V_1 domain subunits B (Vma2p) and C (Vma5p).

absence of V-ATPase function, this in vivo assay is unable to discriminate between major defects in assembly and relatively subtle effects on subunit interactions which compromise activity. We tested for the effects of site-specific Vma4p mutations on V-ATPase assembly by isolating vacuolar membranes from yeast transformants expressing the mutant polypeptides and probing for the presence of subunits B (Vma2p) and C (Vma5p) on the membrane (Figure 7). Deletion of *VMA4* resulted in failure to assemble Vma5p on the vacuolar membrane, consistent with previous reports (*22*, *27*, *33*). However, in contrast to previous reports, we did consistently observe very low levels of Vma2p associated with the membrane in the *VMA4*-deleted mutant (Figure 7), suggesting some residual assembly of a nonfunctional complex, or nonspecific association with the membrane. Transformation of the deletion strain with a cDNA for wild-type *VMA4* restored the ability of subunits B and C to associate with the membrane, indicating assembly of the V-ATPase (Figure 7). We also compared the V-ATPase assembly supported by forms of Vma4p carrying dysfunctional mutations (listed in Table 1) to that supported by the wild-type Vma4p and the functional Leu^{8}→Asp and Thr^{9}→Ala mutants. Although they blocked V-ATPase function in the complementation assay, the Val^{13}→Asp, Leu^{17}→Glu, and Lys^{19}→Glu mutations and Δ1−19 truncation had no significant effect on V-ATPase assembly: high levels of both Vma2p and Vma5p were associated with the vacuolar membranes from strains expressing these forms of Vma4p

```
S.cerevisiae   MSSAITALTPNQVNDELNKMQAFIRKEAEEKAKEIQLKADQEYEIEKTNIVRNETNNIDGNFKSKLKKAM
Candida            MALSDEQVKSELSKMQAFIEKEAKEKAKEIKLKADEEYEIEKASIVRSETAAIDSTYEQKLKKAS
Neurospora      MSQVHALSDDQVGQELRKMTAFIKQEAEEKAREIQIKADEEFAIEKSKLVRQETDAIDSAYAKKFKQAQ
Sch.pombe          MSLSDEQVQAEMHKMVSFIKQEALEKAKEIHTLSEEEFQVEKAKIVREQCDAIDQTYDMKLKRAS
Drosophila         MALSDADVQKQIKHMMAFIEQEANEKAEEIDAKAEEEFNIEKGRLVQQQRLKIMEYYEKKEKQVE
Bovine             MALSDADVQKQIKHMMAFIEQEANEKAEEIDAKAEEEFNIEKGRLVQTQRLKIMEYYEKKEKQIE
Human              MALSDADVQKQIKHMMAFIEQEANEKAEEIDAKAEEEFNIEKGRLVQTQRLKIMEYYEKKEKQIE
Manduca            MALSDADVQKQIKHMMAFIEQEANEKAEEIDAKAEEEFNIEKGRLVQQQRLKIMEYYEKKEKQVE
Consensus           AL*   V   * *M AFI *EA EKA EI  K** E* *EK  *V      I      K K
```

FIGURE 8: Aligned sequences of V-ATPase subunit E polypeptides from eukaryotes. Sequences were aligned using BLAST, with the regions corresponding to the N-terminal 70 residues of *Saccharomyces* Vma4p shown. The section between Leu^{8} and Met^{20} of the *Saccharomyces* sequence (black box) represents a major binding site for Vma5p. The highly conserved region extending to Lys^{38} (open box) contributes strongly to the interaction with Vma10p.

Table 1: Effects of *VMA4* Mutations on V-ATPase Function in Vivo[a]

mutant	growth at pH 7.5	mutant	growth at pH 7.5	mutant	growth at pH 7.5
Δ*VMA4*	−	$Thr^{9}\rightarrow Asp$	+++	$Glu^{16}\rightarrow Ala$	+++
WT *VMA4*	+++	$Pro^{10}\rightarrow Ala$	+++	$Glu^{16}\rightarrow Lys$	+++
Δ1−19	−	$Asn^{11}\rightarrow Ala$	+++	$Leu^{17}\rightarrow Asp$	−
Δ1−38	−	$Gln^{12}\rightarrow Ala$	+++	$Asn^{18}\rightarrow Ala$	+++
Δ1−69	−	$Val^{13}\rightarrow Asp$	−	$Lys^{19}\rightarrow Ala$	+++
$Leu^{8}\rightarrow Asp$	+	$Asn^{14}\rightarrow Ala$	++	$Lys^{19}\rightarrow Glu$	−
$Thr^{9}\rightarrow Ala$	+++	$Asp^{15}\rightarrow Ala$	+++	$Met^{20}\rightarrow Ala$	−

[a] The effect of individual mutations or truncations was determined using the complementation assay outlined in Figure 6. *Saccharomyces* cells were transformed with pYES2 plasmids harboring cDNAs for each mutated or truncated form of *VMA4*, and growth monitored on yeast extract-peptone plates buffered to pH 7.5 and supplemented with galactose and raffinose. Growth at pH 7.5, indicative of restored V-ATPase function, was scored relative to that of the strain transformed with wild-type *VMA4* (+++). + indicates very weak growth; − indicates no growth at pH 7.5.

(Figure 7). Only the $Met^{20}\rightarrow Ala$ mutation had a differential effect on assembly of the two polypeptides, with normal levels of Vma2p but no Vma5p assembled on the membrane. Because a Vma4p polypeptide is requisite for any significant V-ATPase assembly (*22*, *27*), we can conclude that the mutant Vma4p polypeptides must be expressed and correctly folded in the yeast cells. The mutations that prevent the V-ATPase from operating in vivo must have relatively small, subtle effects on subunit interaction. Nevertheless, these are expressed as dramatic effects on function.

DISCUSSION

Although the precise functions of Vma4p and Vma5p remain uncertain, studies with yeast mutants deleted for the corresponding *VMA* gene have provided clues about their roles. Thus, Vma4p appears to be a core component of the V-ATPase "motor", with deletion reported to result in complete failure to assemble the V-ATPase (*27*). In contrast, deletion of *VMA5* still permits assembly of an apparently normal membrane domain, an inactive cytoplasmic V_1 domain, and even some inactive/unstable V-ATPase, although expression of Vma5p is required for full activity (*22*, *33*). Vma5p in yeast therefore appears to be specifically involved in controlling the functional coupling between soluble and membrane domains (*33*). This study shows that the N-terminal 19 amino acid region of Vma4p is a key determinant in the direct interaction of Vma4p with Vma5p in vitro. Given the strength and specificity of this interaction, one might expect it to be a key factor in assembly of the active V-ATPase in vivo. Despite this, it is clear that Vma4p mutations that disrupt Vma5p−Vma4p interaction in vitro do not prevent Vma5p from becoming integrated into the V-ATPase in vivo (Figure 7). However, it is equally clear that these mutations do result in loss of V-ATPase function (Table 1). Our hypothesis is that the Vma4p mutations that compromise V-ATPase function do disrupt an interaction with Vma5p, which is crucial for V-ATPase activity, but that interactions between Vma5p and other subunits maintain the presence of Vma5p in the assembled but inactive enzyme. Indeed, considering the proposed role for Vma5p in coupling the soluble and membrane domains, multiple interactions are extremely likely. Effects on Vma4p−Vma5p association in vitro are mediated primarily via leucine, valine, and methionine residues (Figure 5), suggesting that association between these polypeptides is based on hydrophobic interaction. This is consistent with mutagenesis studies performed on Vma5p, which have pointed to the importance of a C-terminal hydrophobic region in stabilizing interaction with the V_1 domain (*34*). It is also interesting to note that alignment of sequences of subunit E from eukaryotes with those of prokaryotic homologues (*35*, *36*) show that the bacterial polypeptides are truncated at the N-terminus and are therefore missing the majority of residues which appear to be involved in mediating Vma5p/Vma4p interaction. These prokaryotic V-ATPases do not have a Vma5p (subunit C) equivalent.

In *Saccharomyces*, rapid but reversible dissociation of V_1 from the membrane occurs during glucose starvation, causing Vma5p to become detached from the otherwise stable and intact V_1 domain (*37*). Specific loss of Vma5p implies that it plays a role in this mechanism of reversible decoupling. It has recently been reported that Vma4p also interacts with Rav1p, a component of the RAVE complex that associates with free cytoplasmic V_1 domains and is involved in regulating V-ATPase assembly (*38*, *39*). The possibility that the interaction between Rav1p and Vma4p in cytoplasmic V_1 domains occurs at the expense of the Vma4p/Vma5p interaction is attractive, but requires further investigation.

The interaction between Vma4p and Vma10p, previously recognized because the two polypeptides form a subcomplex

in vivo (*21*), was further resolved in this study. A region of Vma4p between residues 19 and 38, which contains a series of highly conserved sequence motifs (Figure 8), certainly appears to be involved in binding Vma10p. This region is highly enriched in charged residues, with the extended sequence between residues Met^{20} and Lys^{38} containing 14 charged residues, of which 9 are almost universally conserved among eukaryotic species (Figure 8). It is interesting to note that Vma10p also contains an unusually high proportion of charged amino acids (see, for example, ref *11*). There may therefore be a role for short-range electrostatics in maintaining either Vma4p/Vma10p interactions, Vma10p dimerization (see Figure 2; *31*), or both. Clues about which region of Vma10p might contact Vma4p come from mutational studies that have shown that Vma10p mutations within the Tyr^{46}−Lys^{55} region destabilize the interaction with Vma4p (*40*). This 10-residue block contains six charged residues.

Further clues about the orientation of Vma10p with respect to the V_1 domain may be found by drawing parallels with the organization of the stator structure within the *E. coli* F-ATPase. The extreme C-terminus of subunit b is close to the region of the F_1-soluble domain furthest from the membrane (*19*). Given the apparent evolutionary relationship between Vma10p and subunit b (*11*), it is reasonable to suppose that the V-ATPase subunit adopts a similar configuration. In the F-ATPase, subunit b makes contacts with both β- and α-subunits (*41*). In particular, a site within subunit b that is equivalent to residue Ala^{72} of Vma10p (*11*) cross-links to the α-subunit at a region bounded by residues 102−106 (*41*). The sequence similarity between subunits A and B of the V-ATPase and subunits β and α of the F-ATPase (*8*) means that these core components of the V_1 domain can be modeled on the 3D structures of the F_1-ATPase with a high degree of confidence (see, for example, ref *24*). Models generated using this approach indicate that the region of Vma2p between its second and third methionine residues (Met^{108} and Met^{150}) maps directly onto the region of the α-subunit, which binds subunit b (Harrison, M. A., unpublished). It is the loss of this region that we suggest results in a failure of GST-Vma10p to bind Vma2p in vitro (Figure 2, lower panel). On this basis, we can therefore speculate that a region of Vma10p close to Ala^{72} contacts this extended loop region of Vma2p, although this clearly requires explicit testing.

Despite a lack of sequence similarity between subunit E/Vma4p of the V-ATPase and the δ-subunit of the *E.coli* F-ATPase, the two polypeptides do appear to show remarkable convergence with regard to their positions within the F- and V-ATPase complexes. While the δ-subunit cross-links to both the α-subunit (*42*) and the b-subunit (*19*, *43*, *44*), Vma4p binds to sites distributed across the surface of Vma2p (*24*) and Vma10p (*21*). In this study, we have identified the N-terminal region of Vma4p as a key site in binding not only Vma10p, but also Vma5p. The 70-residue N-terminal region of Vma4p is also reported to be crucial in binding Vma13p (*23*). This subunit, required for activity, but not assembly of the V-ATPase, also acts to silence ATP hydrolysis by cytosolic V_1 domains released as a result of glucose deprivation (*37*, *38*, *45*). The N-terminal 70-residue region of Vma4p therefore performs two quite distinct functions. It not only maintains stable interactions with core subunits within the stator structure of the V-ATPase in a way that parallels the organization of the F-ATPase, but it also makes functionally crucial interactions with Vma5p and Vma13p, subunits with apparent regulatory functions which are specialized components unique to the V-type enzyme. A more detailed picture of subunit interactions will help our understanding of the structure of the stator element of the V-ATPase motor, in particular, how linkages within the stator structure are able to accommodate the relatively large-scale conformational changes and physical strains associated with the cycle of ATP hydrolysis. It may also provide structural insights into the mechanisms that influence these interactions in response to physiological factors such as changes in carbon source supply.

REFERENCES

1. Nishi, T., and Forgac, M. (2002) The vacuolar (H+)-ATPases − Nature's most versatile proton pumps, *Nat. Rev. Mol. Cell Biol. 3*, 94−103.
2. Stevens, T. H., and Forgac, M. (1997) Structure, function and regulation of the vacuolar (H+)-ATPase, *Annu. Rev. Cell Dev. Biol. 13*, 779−808.
3. Hirata, T., Iwamoto-Kihara, A., Sun-Wada, G. H., Okajima, T., Wada, Y., and Futai, M. (2003) Subunit rotation of vacuolar-type proton pumping ATPase: relative rotation of the g and c subunits, *J. Biol. Chem. 278*, 23714−23719.
4. Imamura, H., Nakano, M., Noji, H., Muneyuki, E., Ohkuma, S., Yoshida, M., and Yokoyama, K. (2003) Evidence for rotation of V_1-ATPase, *Proc. Natl. Acad. Sci. U.S.A. 100*, 2312−2315.
5. Kinosita, K., Yasuda, R., Noji, H., Ishiwata, S., and Yoshida, M. (1998) F_1-ATPase: a rotary motor made of a single molecule, *Cell 93*, 21−24.
6. Arai, A., Terres, G., Pink, S., and Forgac, M. (1988) Topography and subunit stoichiometry of the coated vesicle proton pump, *J. Biol. Chem. 263*, 8796−8802.
7. Forgac, M. (1998) Structure, function and regulation of the vacuolar (H^+)-ATPases, *FEBS Lett. 440*, 258−263.
8. Bowman, E. J., Tenney, K., and Bowman, B. J. (1988) Isolation of genes encoding the Neurospora vacuolar ATPase: analysis of vma1 encoding the 67 kDa subunit reveals homology to the other ATPases, *J. Biol. Chem. 263*, 13994−14001.
9. Zimniak, L., Dittrich, P., Gogarten, J. P., Kibak, H., and Taiz, L. (1988) The cDNA sequence of the 60 kDa subunit of carrot vacuolar ATPase, *J. Biol. Chem. 263*, 9102−9112.
10. Mandel, M., Moriyama, Y., Hulmes, J. D., Pan, Y.-C. E., Nelson, H., and Nelson, N. (1988) cDNA sequence encoding the 16-kDa proteolipid of chromaffin granules implies gene duplication in the evolution of H^+-ATPases, *Proc. Natl. Acad. Sci. U.S.A. 85*, 5521−5524.
11. Hunt, I. E., and Bowman, B. J. (1997) The intriguing evolution of the b and G subunits in F-type and V-type ATPases: Isolation of the vma-10 gene from *Neurospora crassa*, *J. Bioenerg. Biomembr. 29*, 533−540.
12. Supekova, L., Supek, F., and Nelson, N. (1995) The *Saccharomyces cerevisiae VMA10* is an intron-containing gene encoding a novel 13-kDa subunit of vacuolar H(+)-ATPase, *J. Biol. Chem. 270*, 13726−13732.
13. Noji, H., Yasuda, R., Yoshida, M., and Kinosita, K. (1997) Direct observation of the rotation of F-1-ATPase, *Nature 386*, 299−302.
14. Gruber, G., Godovac-Zimmermann, J., Link, T. A., Coskun, U., Rizzo, V. F., Betz, C., and Bailer, S. M. (2002) Expression, purification, and characterisation of subunit E, an essential subunit of the vacuolar ATPase, *Biochem. Biophys. Res. Commun. 298*, 383−391.
15. Jones, R. P. O., Hunt, I. E., Jaeger, J., Ward, A., O'Reilly, J., Barratt, E., Findlay, J. B. C., and Harrison, M. A. (2001) Expression, purification and secondary structure analysis of *Saccharomyces cerevisiae* vacuolar membrane H+-ATPase subunit F (Vma7p), *Mol. Membr. Biol. 18*, 283−290.
16. Tanabe, M., Nishio, K., Iko, Y., Sambongi, Y., Iwamoto-Kihara, A., Wada, Y., and Futai, M. (2001) Rotation of a complex of the gamma subunit and c ring of *Escherichia coli* ATP synthase. The rotor and stator are interchangeable, *J. Biol. Chem. 276*, 15269−15274.

17. Yokoyama, K., Nakano, M., Imamura, H., Yoshida, M., and Tamakoshi, M. (2003) Rotation of the proteolipid ring in the V-ATPase, *J. Biol. Chem. 278*, 24255.
18. Wilkens, S., Vasilyeva, E., and Forgac, M. (1999) Structure of the vacuolar ATPase by electron microscopy, *J. Biol. Chem. 274*, 31804−31810.
19. Rodgers, A. J. W., and Capaldi, R. A. (1998) The second stalk composed of the b- and delta-subunits connects F_0 to F_1 via and alpha-subunit in the *Escherichia coli* ATP synthase. *J. Biol. Chem. 273*, 29406−29410.
20. Xu, T., Vasilyeva, E., and Forgac, M. (1999) Subunit interactions in the clathrin-coated vesicle vacuolar (H^+)-ATPase complex, *J. Biol. Chem. 274*, 28909−28915.
21. Tomashek, J. J., Graham, L. A., Hutchins, M. U., Stevens, T. H., and Klionsky, D. J. (1997) V-1-situated stalk subunits of the yeast vacuolar proton-translocating atpase. *J. Biol. Chem. 272*, 26787−26793.
22. Puopolo, K., Sczekan, M., Magner, R., and Forgac, M. (1992) The 40-kDa subunit enhances but is not required for activity of the coated vesicle proton pump, *J. Biol. Chem. 267*, 5171−5176.
23. Lu, M., Vergara, S., Zhang, L., Holliday, L. S., Aris, J., and Gluck, S. L. (2002) The amino-terminal domain of the E subunit of vacuolar H^+-ATPase (V-ATPase) interacts with the H subunit and is required for V-ATPase function, *J. Biol. Chem. 277*, 38409−38415.
24. Arata, Y., Baleja, J. D., and Forgac, M. (2002) Cysteine-directed cross-linking to subunit B suggests that subunit E forms part of the peripheral stalk of the vacuolar H^+-ATPase, *J. Biol. Chem. 277*, 3357−3363.
25. Ito, H., Fukuda, Y., Murata, K., and Kimura, A. (1983) Transformation of intact yeast-cells treated with alkali cations. *J. Bacteriol. 153*, 163−168.
26. Nelson, H., and Nelson, N. (1990) Disruption of genes encoding subunits of yeast vacuolar H^+-ATPase causes conditional lethality, *Proc. Natl. Acad. Sci. U.S.A. 87*, 3503−3507.
27. Ho, M. N., Hill, K. J., Lindorfer, M. A., and Stevens, T. H. (1993) Isolation of vacuolar membrane H^+ATPase deficient mutants: the VMA4 and VMA5 genes are essential for assembly and activity of the vacuolar H^+ATPase, *J. Biol. Chem. 268*, 221−227.
28. Uchida, E., Ohsumi, Y., and Anraku, Y. (1985) Purification and properties of H^+-translocating, Mg^{2+}-adenosine triphosphatase from vacuolar membranes of *Saccharomyces cerevisiae*, *J. Biol. Chem. 260*, 1090−1095.
29. Kane, P. M., Yamashiro, C. T., Wolcczyk, D. F., Neff, N., Goebl, M., and Stevens, T. H. (1990) Protein splicing converts the yeast TFP1 gene product to the 69-kD subunit of the vacuolar H+-adenosine triphosphatase, *Science 250*, 651−657.
30. Harrison, M. A., Durose, L., Song, C. F., Barratt, E., Trinick, J., Jones, R., and Findlay, J. B. C. (2003) Structure and function of the vacuolar H+-ATPase: moving from low resolution models to high-resolution structures, *J. Bioenerg. Biomembr. 35*, 337−345.
31. Armbruster, A., Bailer, S. M., Koch, M., Godovac-Zimmermann, J., and Grüber, G. (2003) Dimer formation of subunit G of the yeast V-ATPase, *FEBS Lett. 546*, 395−400.
32. Cuff, J. A., Clamp, M. E., Siddiqui, A. S., Finlay, M., and Barton, G. J. (1998) JPred: a consensus secondary structure prediction server, *Bioinformatics 14*, 892−893.
33. Doherty, R. D., and Kane, P. M. (1993) Partial assembly of the yeast vacuolar H(+)-ATPase in mutants lacking one subunit of the enzyme, *J. Biol. Chem. 268*, 16845−16851.
34. Curtis, K., Francis, S. A., Oluwatosin, Y., and Kane, P. M. (2002) Mutational analysis of the subunit C (Vma5p) of the yeast vacuolar H^+-ATPase, *J. Biol. Chem. 277*, 8979−8988.
35. Takase, K., Kakinuma, S., Yamato, I., Konishi, K., Igarashi, K., and Kakinuma, Y. (1994) Sequencing and characterisation of the ntp gene cluster for vacuolar-type Na^+-translocating ATPase of *Enterococcus hirae*, *J. Biol. Chem. 269*, 11037−11044.
36. Yokoyama, K., Akabane, Y., Ishii, N., and Yoshida, M. (1994) Isolation of prokaryotic V_0V_1-ATPase from a thermophilic eubacterium *Thermus thermophilus*, *J. Biol. Chem. 269*, 12248−12253.
37. Kane, P. M. (1995) Disassembly and reassembly of the yeast vacuolar H(+)-ATPase in vivo, *J. Biol. Chem. 270*, 17025−17032.
38. Smardon, A. M., Tarsio, M., and Kane, P. M. (2002) The RAVE complex is essential for stable assembly of the yeast V-ATPase, *J. Biol. Chem. 277*, 13831−13839.
39. Seol, J., Shevchenko, A., Shevchenko, A., and Deshaies, R. (2001) Skp1 forms multiple protein complexes, including RAVE, a regulator of V-ATPase assembly, *Nat. Cell Biol. 3*, 384−391.
40. Charsky, C. M. H., Schumann, N. J., and Kane, P. M. (2000) Mutational analysis of subunit G (Vma10p) of the yeast vacuolar H^+-ATPase, *J. Biol. Chem. 275*, 37232−37239.
41. McLachlin, D. T., Coveny, A. M., Clark, S. M., and Dunn, S. D. (2000) Site-directed cross-linking of b to the alpha, beta, and a subunits of the *Escherichia coli* ATP synthase, *J. Biol. Chem. 275*, 17571−17577.
42. Ogilvie, I., Aggeler, R., and Capaldi, R. A. (1997) Cross-linking of the delta subunit to one of the three alpha subunits has no effect on functioning, as expected if delta is a part of the stator that links the F_1 and F_0 parts of the *Escherichia coli* ATP synthase, *J. Biol. Chem. 272*, 16652−16656.
43. Rodgers, A. J. W., Wilkens, S., Aggeler, R., Morris, M. B., Howitt, S. M., and Capaldi, R. A. (1997) The subunit delta-subunit b domain of the *Escherichia coli* F_1F_0-ATPase, *J. Biol. Chem. 272*, 31058−31064.
44. Sawada, K., Kuroda, N., Watanabe, H., Moritani-Otsuka, C., and Kanazawa, H. (1997) Interaction of the delta and b subunits contributes to F_1 and F_0 interaction in the *Escherichia coli* F_1F_0-ATPase, *J. Biol. Chem. 272*, 30047−30053.
45. Parra, K. J., Keenan, K. L., and Kane, P. M. (2000) The H subunit (Vma13p) of the yeast V-ATPase inhibits the ATPase activity of cytosolic V_1 complexes, *J. Biol. Chem. 275*, 21761−21767.

BI048402X